

Black hole singularities: a numerical approach

Patrick R. Brady* and John D. Smith

*Department of Physics, The University, Newcastle Upon Tyne NE1 7RU
(4 April 1995)*

The singularity structure of charged spherical collapse is studied by considering the evolution of the gravity-scalar field system. A detailed examination of the geometry at late times strongly suggests the validity of the mass-inflation scenario [3]. Although the area of the two-spheres remains finite at the Cauchy horizon, its generators are eventually focused to zero radius. Thus the null, mass-inflation singularity *generally* precedes a crushing $r = 0$ singularity deep inside the black hole core. This central singularity is spacelike.

PACS: 04.40.Nr, 02.60.Cb, 97.60Lf, 04.20Dw

The radiative tail of gravitational collapse decays as an inverse power of time leaving behind a black hole characterized only by its mass, charge and angular momentum [1]. The simplicity of the external field at late times contrasts with the highly dynamical interior which lies beneath the event horizon [2,3,4,5].

It is generally accepted that the “tunnel” through a charged or rotating black hole is destroyed by perturbations which propagate into the hole after its formation [6,7]. The manner in which this occurs has been studied in great detail using simplified models [2,3,4,5], and the results suggest that the Cauchy horizon (CH) inside a charged (or rotating) black hole is transformed into a singularity at which the “Coulomb” component of the Weyl curvature diverges. The null generators of the CH contract slowly under transverse irradiation, so it is anticipated that this null singularity eventually gives way to a central spacelike singularity deep inside the black hole core. It should be noted that this spacelike singularity is *not* expected to precede the CH as some authors have argued [8,9]. Indeed, geodesic observers falling into the black hole at late times will generally encounter only the null singularity.

Some disquiet exists regarding this picture of the black hole interior. Yurtsever [8] has argued, on general grounds, that complete destruction of the CH should be expected once generic perturbations are considered. He bases his discussion on experience with colliding plane wave spacetimes — he has shown that plane wave Cauchy horizons are replaced by spacelike singularities in the presence of generic plane-symmetric perturbations [10]. Gnedin and Gnedin [9], on the other hand, have performed a numerical integration of the spherical Einstein-Maxwell-scalar field equations. They established the existence of a spacelike singularity inside a charged black hole coupled with scalar matter. Their analysis stressed the behaviour of the central ($r = 0$) singularity, however they did not consider the possibility that it intersects the Cauchy horizon.

This letter reports on an independent numerical investigation. We find evidence that the analytic models

demonstrate the essential features of black hole internal structure.

The general spherical line element can be written as

$$ds^2 = -g\bar{g}dv^2 - 2gdvdr + r^2(d\theta^2 + \sin^2\theta d\phi^2), \quad (1)$$

where $g = g(r, v)$, $\bar{g} = \bar{g}(r, v)$ and v is advanced time. We solve the field equations $G_{\alpha\beta} = 8\pi(E_{\alpha\beta} + T_{\alpha\beta})$ where

$$E^\alpha_\beta = (e^2/8\pi r^4) \text{diag}(-1, -1, 1, 1) \quad (2)$$

is the standard electromagnetic contribution to the stress-energy, and

$$4\pi T_{\alpha\beta} = \phi_{,\alpha}\phi_{,\beta} - \frac{1}{2}g_{\alpha\beta}(\phi_{,\gamma}\phi^{,\gamma}) \quad (3)$$

is the stress energy for a massless, minimally coupled scalar field ϕ . It is convenient to write $\bar{h} = \phi$ and then introduce the scalar $h(r, v)$ by

$$(r\bar{h})_{,r} = h. \quad (4)$$

The field equations can now be written as

$$(\ln g)_{,r} = r^{-1}(h - \bar{h})^2, \quad (5)$$

$$(r\bar{g})_{,r} = g(1 - e^2/r^2), \quad (6)$$

while the wave equation $\square\phi = 0$ becomes

$$h_{,v} - \frac{\bar{g}}{2}h_{,r} = \frac{1}{2r}(h - \bar{h})(g[1 - e^2/r^2] - \bar{g}). \quad (7)$$

The pioneering numerical integration of these equations, with $e = 0$, was performed by Goldwirth and Piran [11]. We have employed a similar algorithm. Using the method of characteristics Eq. (7) is recast as a set of $2n$ ordinary differential equations, where n is the number of radial grid points. The radial integrals in Eq. (4)-Eq. (6) are discretized according to the trapezium rule, while we use a Runge-Kutta scheme for the ordinary differential equations. The resulting code is locally second order accurate, and has been tested on Reissner-Nordström spacetime and the exact self-similar solutions in [12]. The details will appear elsewhere.

To aid the comparison to previous work [3,4] we introduce the mass function

$$m(x^\alpha) = \frac{r}{2} (1 + e^2/r^2 - \bar{g}/g) . \quad (8)$$

Moreover the sole non-vanishing Newman-Penrose Weyl scalar

$$-\Psi_2 = \frac{1}{2} C^{\theta\phi} \theta_\phi = [m(x^\alpha) - e^2/r] r^{-3} , \quad (9)$$

is simply expressed in terms of this mass function and provides a direct measure of curvature near the CH.

Characteristic initial data are supplied on a pair of intersecting null hypersurfaces as shown in Fig. 1. The spacetime is Reissner-Nordström when $v < v_0$. After this advanced time we consider the evolution of a charged black hole with infalling scalar matter. Since our primary interest is the black hole interior it is useful to choose the outgoing null hypersurface, Γ , coincident with the event horizon. This is achieved by first setting $g|_\Gamma = -1$, then specifying $r|_\Gamma$ such that

$$\lim_{v \rightarrow \infty} r|_\Gamma = \text{constant} . \quad (10)$$

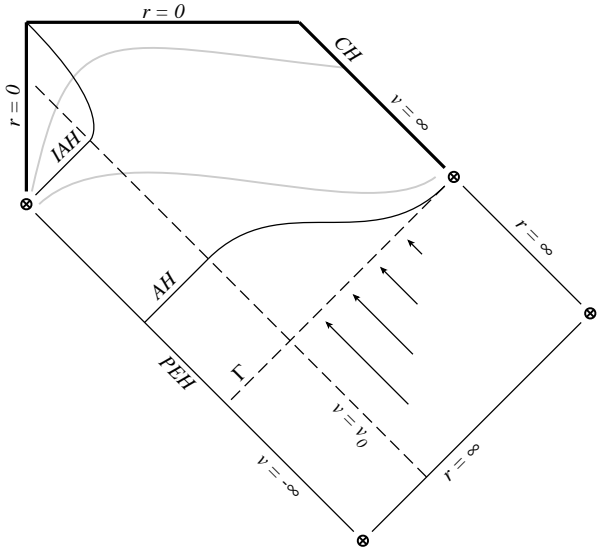


FIG. 1. A spacetime diagram showing the setting of the numerical integration. The spacetime is Reissner-Nordström for $v < v_0$. Scalar field falls into the black hole across the event horizon, Γ . PEH is the past event horizon, located at $v = -\infty$. AH is the outer apparent horizon, and IAH is the inner apparent horizon of the charged black hole. A couple of lines of constant r are shown in light gray. The Cauchy horizon (CH) is a singular hypersurface which contracts to meet the central singularity at $r = 0$. All singularities are indicated by thick lines in the diagram.

The dynamical equations (4)-(7) are supplemented by one further equation along each outgoing null hypersurface:

$$\frac{d\bar{g}}{dv} = \bar{g} \left(\frac{d \ln g}{dv} - \frac{1}{2r^3} [g(r^2 - e^2) - \bar{g}] \right) + 2r \left(\frac{d\phi}{dv} \right)^2 . \quad (11)$$

This is Raychaudhuri's equation for the outgoing null rays, and is conserved by the evolution. Using the characteristic equation $dr/dv = -\bar{g}/2$ to obtain $\bar{g}|_\Gamma$, it is straightforward to integrate Eq. (11) along Γ , with the appropriate initial conditions at $v = v_0$, for $\phi|_\Gamma$.

Beneath the event horizon of the black hole outgoing null rays contract rapidly (see Fig. 2). Consequently an initially uniform radial grid becomes highly non-uniform at late times, leading to significant errors in \bar{g} . We have employed a non-uniform grid along the initial ingoing null ray to alleviate this problem, making the radial grid points more dense in the vicinity of the event horizon. A significant increase in (accurate) integration time is obtained by this method, and the internal mass function [defined in Eq. (8)] reaches values up to about 10^{50} times the external black hole mass before errors become significant.

We have integrated the equations for several choices of initial data along Γ , and have obtained the same qualitative behaviour. Table I summarizes the results obtained for the two initial data sets characterized by

$$r|_\Gamma = \begin{cases} r_+ - \beta v^{-p} \\ r_+ - \beta \exp(-pv^2) \end{cases} \quad (12)$$

where $\beta > 0$ and $p > 0$ are real parameters. It is convenient to fix dimensions such that the asymptotic Bondi mass is unity, thus the radius of the event horizon approaches $r_+ = 1 + \sqrt{1 - e^2}$ as $v \rightarrow \infty$. The inverse power-law data along Γ is taken as representative of the physical situation where the flux of radiation across the event horizon exhibits such a decay [13]. We have included the second data set to emphasize that the non-linear instability of the inner horizon is present even for perturbations having compact support on the event horizon. This result should be expected based on linear analysis of the problem [7].

TABLE I. Late time behaviour of the metric along characteristics labelled by u . Multiplicative factors which depend only on u have been omitted. The constants γ , μ , and σ are discussed in the text.

Initial data	$g(u, v)$	$\bar{g}(u, v)$	$m(u, v)$
$r_+ - \beta v^{-p}$	$e^{-\gamma v}$	$v^{-(p+1+\sigma)} e^{\gamma v}$	$v^{-(p+1+\sigma)} e^{\gamma v}$
$r_+ - \beta e^{(-pv^2)}$	$e^{-\gamma v}$	$e^{-2\mu v}$	$e^{(\gamma-2\mu)v}$

In Reissner-Nordström spacetime all outgoing null geodesics which originate inside the black hole intersect the CH within a finite affine parameter. However, the presence of the scalar field modifies the causal structure of the spacetime so that some outgoing null rays terminate at $r = 0$ in a finite coordinate time v (i.e. before

intersecting the CH). This important result is demonstrated in Fig. 2, which shows the radius as a function of external advanced time along a selection of outgoing null rays. In this coordinate system the lightcones tip over at $r = 0$ indicating that the singularity at this hypersurface is spacelike.

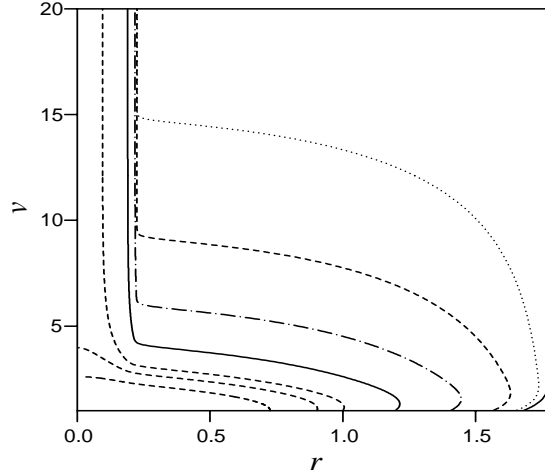


FIG. 2. The null rays in the rv -plane. The inner-most rays terminate at $r = 0$ in a finite advanced time, however there exist many geodesics which approach a finite radius at large v . Subsequent figures show \bar{g} and g along the five outermost rays indicated by different line types. The initial data is exponential with $\beta = 0.26$, $p = 1$ and $e^2 = 0.4$.

Generally we have found the outgoing null rays to belong to two distinct classes, those which reach $r = 0$ and those which do not. The latter geodesics are of greatest interest to us here and below. Each member of this class approaches a fixed radius at late times, indicating the existence of a CH in these solutions. Notice that the final radius is different for each geodesic; the CH is not a stationary null hypersurface, as it is in Reissner-Nordström spacetime, rather it contracts slowly under transverse irradiation. Moreover, the CH is the locus of a null, precursory singularity which precedes the crushing singularity at the origin (see Fig. 1). Gnedin and Gnedin examined only the central singularity in [9], overlooking the existence of the null portion.

One might worry that the cumulative effect of infalling scalar field could eventually focus all outgoing null rays to zero radius. To allay such doubts we have examined the expansion rate $\bar{g} = -2 dr/dv$ along outgoing null rays. Typically \bar{g} reaches a maximum along each geodesic, then it exhibits a period of exponential decay followed by a less pronounced, but definite, approach to zero which is characteristic of the initial data (see Fig. 3). Table I gives the form of \bar{g} for large v , demonstrating that the assumptions used in asymptotic calculations are valid [5,14].

Our initial conditions along Γ reflect the relaxation of the external gravitational field to Reissner-Nordström spacetime at late times. It seems reasonable that this

property should continue to hold inside the event horizon as far as some imprecisely defined radius, where non-linear gravitational effects become important. This expectation is indeed realized in our numerical simulations, justifying the assumption used in [15] to analytically estimate the effects of the scalar field on the charged black hole interior. We find a thick (in terms of r) layer where the presence of scalar matter produces only slight deviations from an exact Reissner-Nordström solution. This effect is most pronounced in the function g at late times; near to the event horizon $g \simeq -1$ as in Reissner-Nordström spacetime, however it rapidly approaches zero beyond this region.

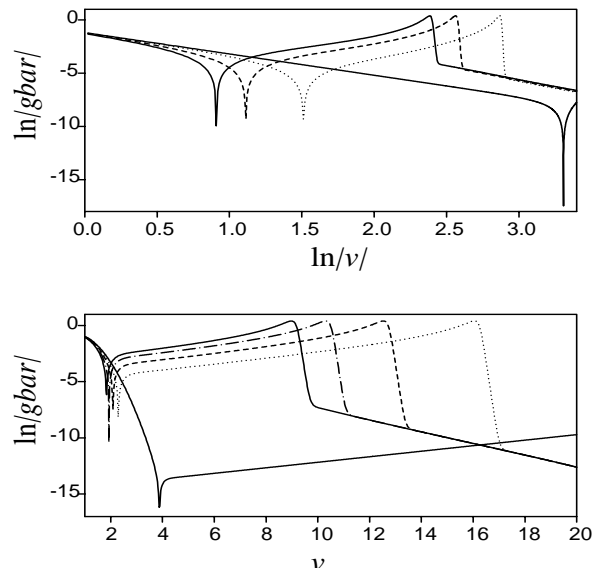


FIG. 3. These plots show $\ln |\bar{g}|$ along a selection of outgoing null rays which intersect the CH. The top graph shows $\ln |\bar{g}|$ against $\ln |v|$ for the inverse power data in Table I. The late time fall-off is clearly a power law too. The graph is $\ln |\bar{g}|$ against v for the exponential data. The linear relation in this graph indicates an exponential fall-off at late times. The cusp in these figures corresponds to a change in the sign of \bar{g} where the outgoing null ray intersects the outer apparent horizon of the black hole.

Figure 4 shows $\ln |g|$ plotted against advanced time along selected null rays. At late times $g \sim e^{-\gamma v}$, where γ depends only on the charge e . We find $\gamma \simeq \kappa_-$ as predicted by analytic models [4], where $\kappa_- = \sqrt{1 - e^2}/(1 - \sqrt{1 - e^2})^2$ is the surface gravity of the inner horizon of a static black hole with equivalent mass and charge. This result holds to within about 10%.

While a suitable coordinate transformation can render the metric non-singular [4], the exponential decrease in g is reflected in the growth of curvature as the CH is approached. In fact $C^{\alpha\beta\gamma\delta}C_{\alpha\beta\gamma\delta} \simeq 48m^2(u, v)/r^6(u, v) \sim \bar{g}^2(u, v)e^{2\gamma v}$ along outgoing null rays. (u labels the outgoing null hypersurfaces on which we have examined the

functions.) For a black hole of about one solar mass we have been able to follow the evolutions to curvatures around Planck levels.

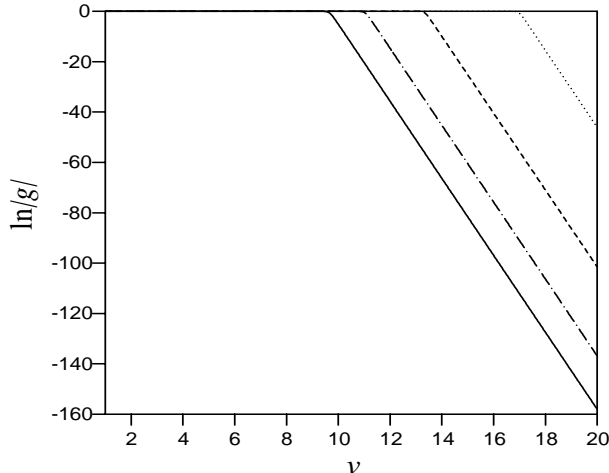


FIG. 4. $\ln|g|$ against advanced time along the outgoing null rays. The asymptotic form $g \sim e^{-\gamma v}$ is in remarkable agreement with predictions based on simplified models.

Analytic models have relied heavily on the results of linear perturbation theory to provide information about energy fluxes along the CH. Therefore, we have examined the flux of scalar field parallel to the CH in our solutions, finding qualitative agreement with perturbative analyses. It is straightforward to see this remarkable feature directly from Raychaudhuri's equation (11) and the results in Table I. If $l^\alpha = dx^\alpha/dv$ is a lightlike generator of the outgoing characteristics then the flux of scalar matter across these surfaces is

$$\mathcal{F} := 4\pi T_{\alpha\beta} l^\alpha l^\beta = (d\phi/dv)^2. \quad (13)$$

Since $r \rightarrow$ constant and $|g|$ decays exponentially at late times, Eq. (11) implies that

$$\mathcal{F} \simeq A\bar{g} + B d\bar{g}/dv \text{ as } v \rightarrow \infty, \quad (14)$$

where A and B generally depend on the outgoing null surface considered. Now, if the flux across the event horizon at late times is $\mathcal{F}|_\Gamma \sim v^{-p-1}$ then $\mathcal{F} \sim \mathcal{F}|_\Gamma v^{-\sigma}$ with $\sigma > 0$, along null rays which intersect the CH. The value of σ (lying in the range $0.3 < \sigma < 0.75$ for the cases we examined) depends on the charge, and differs from predicted values [7,15] by more than the numerical uncertainty. Generally, if $\mathcal{F}|_\Gamma$ decays faster than $\exp[-2\kappa_+ v]$ for large v , then $\mathcal{F} \sim \exp[-2\mu v]$ where $\mu \simeq \kappa_+ = \sqrt{1-e^2}/(1+\sqrt{1-e^2})^2$ (to within less than 10%). The striking agreement with predictions of linearized theory [7] suggests that perturbative arguments [5,15] are actually valid deep inside the black-hole core.

The most significant shortfall in our analysis is the location of the CH at $v = \infty$. So, how close to the CH do

we really get? Without the entire solution (up to and including the CH) it is difficult to quantify this. However, in terms of a Kruskal-like coordinate $V = -e^{-\kappa-v}$ which goes to zero on the CH we have reached values as small as $V = -10^{-150}$ during our integrations. It might seem tempting to choose such an advanced time coordinate *ab initio*, so that the CH is located at a finite coordinate distance \mathcal{V}_{CH} . However a high price is paid for such a choice; in the new coordinates the initial data $\bar{g}|_\Gamma$ and $g|_\Gamma$ become badly behaved as $\mathcal{V} \rightarrow \mathcal{V}_{CH}$ leading to significantly decreased integration times.

In conclusion, we believe that the effects we have described above are representative of the asymptotic structure of the true black hole interior and that a null, mass inflation singularity is present along the CH. Furthermore, the null CH singularity is a precursor of the final spacelike singularity deep within the black-hole core. A detailed account of this work is in preparation.

We are grateful to Ian Moss and Werner Israel for useful discussions. This research was supported in part by the EPSRC.

- [1] C.W. Misner, K.S. Thorne and J.A. Wheeler, *Gravitation* (Freeman, San Francisco 1973).
- [2] W.A. Hiscock, *Phy. Lett.* **83A**, 110 (1981).
- [3] E. Poisson and W. Israel, *Phys. Rev. D* **41**, 1796 (1990).
- [4] A. Ori, *Phys. Rev. Letters* **67**, 789 (1991).
- [5] A. Ori, *Phys. Rev. Letters* **68**, 2117 (1992).
- [6] R. Penrose, in *Battelle Rencontres* (ed. C. M. DeWitt and J. A. Wheeler), W.A. Benjamin, New York 1968 (p. 222); M. Simpson and R. Penrose, *Int. J. Theor. Phys.* **7**, 183 (1973); J.M. McNamara, *Proc. R. Soc. London* **A358**, 499 (1978).
- [7] S. Chandrasekhar and J.B. Hartle, *Proc. R. Soc. London* **A284**, 301 (1982).
- [8] U. Yurtsever, *Class. Quantum Grav.* **10**, L17 (1993).
- [9] M. L. Gnedin and N. Y. Gnedin, *Class. Quantum Grav.* **10**, 1083 (1993).
- [10] U. Yurtsever, *Phys. Rev. D* **36**, 1662 (1987); *Phys. Rev. D* **38**, 1706 (1988); *Phys. Rev. D* **40**, 329 (1989).
- [11] A. Goldwirth and T. Piran, *Phys. Rev. D* **36**, 3575 (1987).
- [12] P.R. Brady, *Class. Quantum Grav.* **11**, 1255 (1994); Y. Oshiro, K. Nakamura and A. Tomimatsu, *Prog. Theor. Phys.* **91**, 1265 (1994).
- [13] R.H. Price, *Phys. Rev. D* **5**, 2419 (1972).
- [14] P.R. Brady and C.M. Chambers, *Phys. Rev. D* **51**, 4177 (1995).
- [15] A. Bonano, S. Droz, W. Israel and S.M. Morsink, preprint Alberta-Thy-35-94, gr-qc/9411050, to appear in *Proc. Roy. Soc.*